

Quenched charmonium spectrum on anisotropic lattices *

CP-PACS Collaboration : A. Ali Khan,^a S. Aoki,^b R. Burkhalter,^{a,b} S. Ejiri,^a M. Fukugita,^c S. Hashimoto,^d N. Ishizuka,^{a,b} Y. Iwasaki,^{a,b} K. Kanaya,^b T. Kaneko,^d Y. Kuramashi,^d K.-I. Nagai,^a M. Okamoto,^b M. Okawa,^d H.P. Shanahan,^{a†} Y. Taniguchi,^b A. Ukawa,^{a,b} and T. Yoshié^{a,b}

^aCenter for Computational Physics, University of Tsukuba, Tsukuba, Ibaraki 305-8577, Japan

^bInstitute of Physics, University of Tsukuba, Tsukuba, Ibaraki 305-8571, Japan

^cInstitute for Cosmic Ray Research, University of Tokyo, Kashiwa 277-8582, Japan

^dHigh Energy Accelerator Research Organization (KEK), Tsukuba, Ibaraki 305-0801, Japan

We present the results of quenched charmonium spectrum for S- and P-states, obtained by a relativistic heavy quark method on anisotropic lattices. Simulations are carried out using the standard plaquette gauge action and a meanfield-improved clover quark action at $a_t^{-1} = 3-6$ GeV with the renormalized anisotropy fixed to $\xi \equiv a_s/a_t = 3$. We study the scaling of our fine and hyperfine mass splittings, and compare with previous results.

1. Introduction

Conventional formalism of lattice QCD fails to describe heavy quarks because $am_Q \gtrsim O(1)$ for charm and bottom quarks on current lattices with $a^{-1} \sim 1-3$ GeV. In heavy hadrons, however, typical scale for the spatial momenta are comparable with that of light hadrons. A momentum with $O(m_Q)$ appears only in the time direction. Therefore, as proposed by Klassen, it is natural to adopt an anisotropic lattice with a small temporal lattice spacing with $a_t m_Q \ll 1$ for a lattice QCD description of heavy hadrons[1,2].

In this report, we present results of our ongoing calculation on the quenched charmonium spectrum using the anisotropic method, which attempts to test the feasibility of this approach.

2. Method and simulation parameters

The gauge action we use is given by

$$S_g = \beta \sum (1/\xi_0 P_{ss'} + \xi_0 P_{st}), \quad (1)$$

where ξ_0 is the bare anisotropy. The renormalized anisotropy, defined by $\xi \equiv a_s/a_t$, can be de-

*Talk presented by M. Okamoto

†address after 15 Sept., 2000: Department of Biochemistry and Molecular Biology, University College London, London, England, UK

Table 1

Simulation parameters. Lattice spacing is fixed by the Sommer scale $r_0 = 0.5$ fm.

β	ξ	ξ_0	c_s	c_t	$a_s^{r_0}$ [fm]	$L^3 \times T$	La_s [fm]
5.7	3	2.35	1.97	2.51	0.202	$8^3 \times 48$	1.61
5.9	3	2.41	1.84	2.45	0.139	$12^3 \times 72$	1.67
6.1	3	2.46	1.76	2.42	0.100	$16^3 \times 96$	1.60

β	$a_t m_{q0}$	ζ	iter/conf	#conf	$c(0)$
5.7	0.320	2.88	100	1000	1.009(6)
5.7	0.253	2.85	100	1000	1.009(7)
5.9	0.144	2.99	100	1000	0.991(8)
5.9	0.090	2.93	100	1000	0.991(8)
6.1	0.056	3.10	200	600	0.980(10)
6.1	0.024	3.03	200	600	0.982(10)

termined by Wilson loops. In this study, we use the result of [3] for $\xi(\xi_0, \beta)$.

For the quark action, we employ an $O(a)$ -improved Wilson-type quark action on an anisotropic lattice[1,2,4]:

$$S_f = \sum_x \{ \bar{\psi}_x \psi_x - K_t [\bar{\psi}_x (1 - \gamma_0) U_{0,x} \psi_{x+\hat{0}}] \}$$

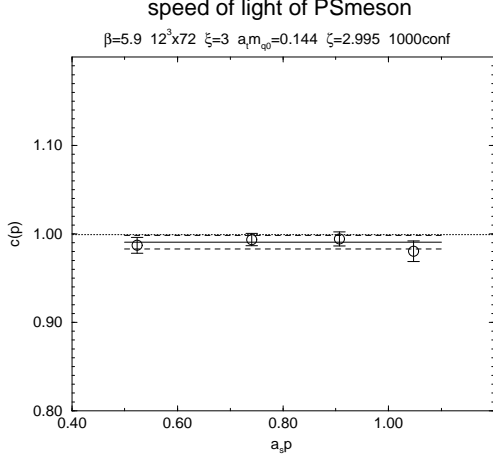


Figure 1. The speed of light and effective speed of light for η_c at tuned ζ and $\beta = 5.9$.

$$\begin{aligned}
& +\bar{\psi}_{x+\hat{0}}(1+\gamma_0)U_{0,x}^\dagger\psi_x] \\
& -K_s\sum_i[\bar{\psi}_x(1-\gamma_i)U_{i,x}\psi_{x+\hat{i}} \\
& +\bar{\psi}_{x+\hat{i}}(1+\gamma_i)U_{i,x}^\dagger\psi_x] \\
& +iK_s c_s\sum_{x,i<j}\bar{\psi}_x\sigma_{ij}F_{ij}(x)\psi_x \\
& +iK_s c_t\sum_{x,i}\bar{\psi}_x\sigma_{0i}F_{0i}(x)\psi_x, \quad (2)
\end{aligned}$$

where $K_{s,t}$ and $c_{s,t}$ are the spatial and temporal hopping parameters and clover coefficients. The bare quark mass is given by

$$a_t m_{q0} = 1/2K_t - 3/\zeta - 1, \quad (3)$$

where $\zeta \equiv K_t/K_s$. We adopt the meanfield-improved clover coefficients:

$$c_s = \frac{1}{\langle U_s \rangle^3}, \quad c_t = \frac{1+\xi}{2} \frac{1}{\langle U_s \rangle \langle U_t \rangle^2}, \quad (4)$$

where $\langle U_s \rangle = \langle P_{ss'} \rangle^{1/4}$ with $P_{ss'}$ the spatial plaquette and $\langle U_t \rangle = 1$.

Our simulation parameters are summarized in Table 1. We study lattices with a fixed renormalized anisotropy $\xi = 3$ and approximately the same spatial lattice size of about 1.6 fm. In order to study the charm quark, we simulate three lattices with the lattice cutoff in the range $a_t^{-1} = 3\text{--}6$ GeV.

The parameter ζ has to be tuned such that the relativistic errors are eliminated. For this purpose

Table 2
S- and P-state operators.

state	J^{PC}	name	local	non-local
1S_0	0^{-+}	η_c	$\bar{\psi}\gamma_5\psi$	
3S_1	1^{--}	J/ψ	$\bar{\psi}\gamma_i\psi$	
1P_1	1^{+-}	h_c	$\bar{\psi}\sigma_{ij}\psi$	$\bar{\psi}\gamma_5\Delta_i\psi$
3P_0	0^{++}	χ_{c0}	$\bar{\psi}\psi$	$\bar{\psi}\sum_i\gamma_i\Delta_i\psi$
3P_1	1^{++}	χ_{c1}	$\bar{\psi}\gamma_i\gamma_5\psi$	$\bar{\psi}\{\gamma_i\Delta_j - \gamma_j\Delta_i\}\psi$
3P_2	2^{++}	χ_{c2}		$\bar{\psi}\{\gamma_i\Delta_j - \gamma_j\Delta_i\}\psi$ (E) $\bar{\psi}\{\gamma_i\Delta_j + \gamma_j\Delta_i\}\psi$ (T)

preparatory simulations are performed at $\zeta = 2.8, 3.0$ and 3.2 . We measure the pseudoscalar meson mass at four lowest on- and off-axis momenta and perform a fit of form,

$$E(p)^2 = E(0)^2 + c^2(p)p^2 \quad (5)$$

to extract the ‘‘speed of light’’, $c(p)$, using three or four lowest momenta. The tuning condition for ζ is $c(p=0) = 1$ which requires the relativistic dispersion relation to be restored for small momenta. (For massless free fermions, $c(p=0) = 1$ is satisfied at $\zeta = \xi$.) Results for ζ are summarized in Table 1.

Figure 1 shows a typical result for the effective speed of light $c_{\text{eff}}(p) = \sqrt{E(p)^2 - E(0)^2}/p$, obtained by a simulation made with a tuned value of ζ . The wide plateau indicates that the linearity of $E(p)^2$ in p^2 is well satisfied. The horizontal solid line is the result of $c(0)$ from a global fit according to (5), where the dashed lines indicate its error. We see that $c(0)$ is consistent with 1. As summarized in Table 1, the condition $c(0) = 1$ is confirmed to be satisfied within 1–2% with our values of ζ .

2.1. Measurements

At each β , hadronic measurements are made on configurations separated by 100–200 iterations, at two values of m_{q0} . See Table 1. These two quark masses are chosen such that the charm quark point can be interpolated.

We measure all S- and P-state mesons using both local and non-local operators compiled in Table 2. For the non-local operators we adopt an

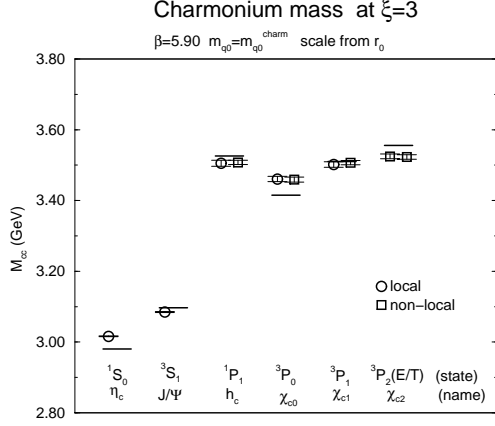


Figure 2. The charmonium mass spectrum at $\xi = 3$ and $\beta = 5.9$. The scale is fixed through the Sommer scale r_0 .

Table 3

Preliminary continuum estimates of mass splittings and the experimental values.

scale	$a_s \rightarrow 0$ r_0	$a_s \rightarrow 0$ ${}^1P_1 - S$	Exp.
$\Delta M_{J/\psi - \eta_c}$ [MeV]	65(1)	82(2)	117
$\Delta M_{\chi_{c1} - \chi_{c0}}$ [MeV]	55(5)	63(5)	95
$\Delta M_{\chi_{c2} - \chi_{c1}}$ [MeV]	19(7)	21(7)	46
$\frac{\Delta M_{\chi_{c2} - \chi_{c1}}}{\Delta M_{\chi_{c1} - \chi_{c0}}}$	0.33(15)	0.31(14)	0.48

exponentially smeared derivative sources:

$$f_i(\mathbf{x}) = A_s e^{-B_s |\mathbf{x} - \hat{i}|} - A_s e^{-B_s |\mathbf{x} + \hat{i}|} \quad (i = 1, 2, 3), (6)$$

where A_s and B_s are the smearing parameters. We extract meson masses by a single cosh fit. Errors are determined by a jack-knife method.

3. Charmonium spectrum

We fix the scale using either the Sommer scale $r_0 = 0.5$ fm or the ${}^1P_1 - 1\bar{S}$ splitting. The charm quark point is then defined by setting the spin averaged $1S$ meson mass ($1\bar{S}$). Figure 2 is a typical result for the charmonium mass spectrum obtained at $\beta = 5.9$. In the following, we study the lattice spacing dependence of the spectrum. With the $O(a)$ improved action, the leading scaling violation is expected to be proportional to a^2 .

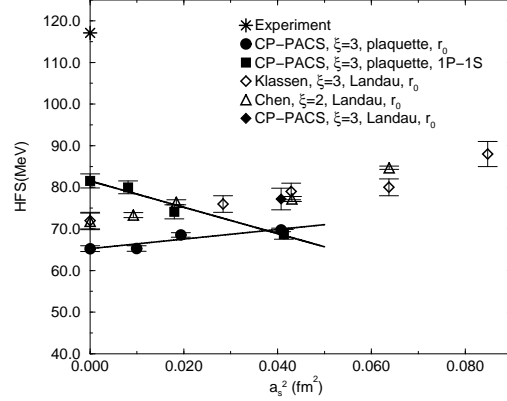


Figure 3. The scaling behavior of hyperfine-splitting $\Delta M_{J/\psi - \eta_c}$. Filled circle and square are our results with scale from the Sommer scale r_0 and the $1P - 1\bar{S}$ splitting respectively. Open diamond and triangle are results of Ref.[2] and [5].

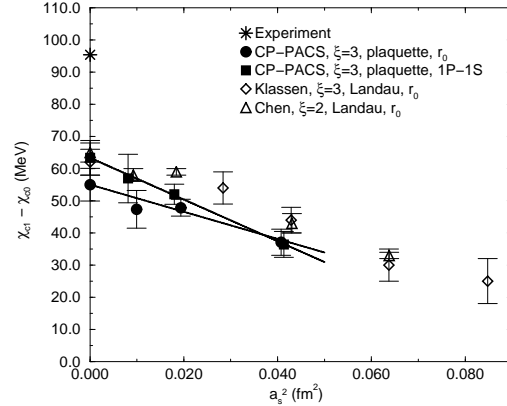
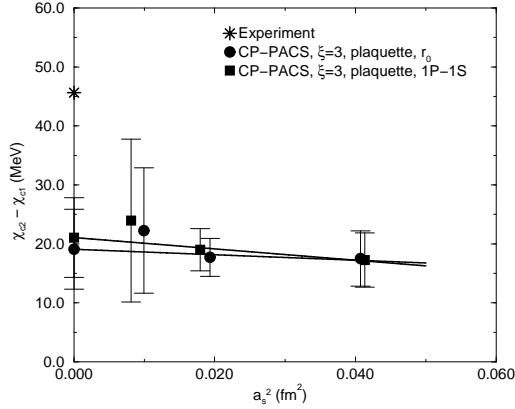
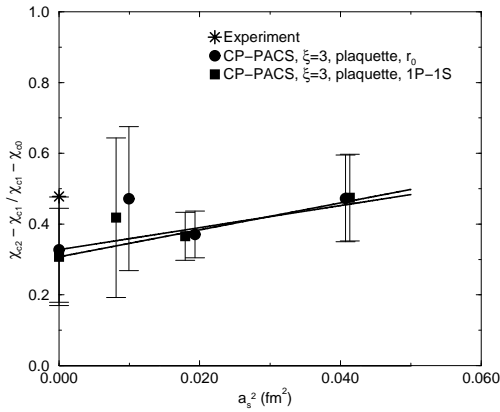


Figure 4. The scaling behavior of $\Delta M_{\chi_{c1} - \chi_{c0}}$.

3.1. Hyperfine splitting

Figure 3 is our result for the S-state hyperfine-splitting $J/\psi - \eta_c$ as a function of the lattice spacing. Results using the scales from r_0 and ${}^1P_1 - 1\bar{S}$ are presented. We find that, although our results for the hyperfine-splitting can be approximately fitted by a linear function of a_s^2 , the two results from different scales lead to different values even in the continuum limit. This discrepancy should be regarded as a quenching artifact.

Plotted together are the previous lattice results by Klassen[2] and Chen[5] at $\xi = 2$ and 3, using the same lattice action. A difference between our

Figure 5. $\Delta M_{\chi_{c2} - \chi_{c1}}$.Figure 6. The ratio $\Delta M_{\chi_{c2} - \chi_{c1}} / \Delta M_{\chi_{c1} - \chi_{c0}}$.

simulation and those in [2] and [5] is the choice of the tadpole factor for the clover coefficients; we use the fourth root of the plaquette expectation value, while the mean link in the Landau gauge is used in [2] and [5]. To check the consistency, we also performed a simulation at $\beta = 5.7$ using the Landau gauge mean link for the meanfield. As shown in Fig. 3 by a filled diamond, our result is consistent with those by Klassen.

We find that our result from the scale r_0 is approximately parallel to the other two results, and lead to a continuum limit which is about 10% lower than that of the others. The origin of this discrepancy is not clear to us at present.

3.2. Fine structure

Results for the P-state fine structure $\chi_{c1} - \chi_{c0}$ are shown in Fig. 4. Although the scaling behavior of our results is similar to those of [2] and [5], the continuum limit deviates by about 2σ for the data using the r_0 scale.

We also show the results for the $\chi_{c2} - \chi_{c1}$ splitting and the ratio $\chi_{c2} - \chi_{c1} / \chi_{c1} - \chi_{c0}$ in Figs. 5 and 6. No data from other groups are available for these quantities.

4. Conclusions

We have presented our results for the charmonium mass spectrum obtained on an anisotropic lattice with $\xi = 3$. Our results for fine and hyperfine mass splittings are shown in Figs.3-6. Our preliminary values from a continuum extrapolation linear in a^2 are summarized in Table 3. We find that these results are much smaller than experimental values.

We also find that the results are quite sensitive to the choice of the clover coefficient. A naive continuum extrapolation, linear in a^2 , does not resolve the discrepancy between different choices of the clover coefficient. We are now extending the simulation to a finer lattice, to examine the reliability of continuum extrapolations.

This work is supported in part by Grants-in-Aid of the Ministry of Education (Nos. 10640246, 10640248, 10740107, 11640250, 11640294, 11740162, 12014202, 12304011, 12640253, 12740133). AAK is supported by JSPS Research for the Future Program (No. JSPS-RFTF 97P01102). SE, TK, KN, M. Okamoto and HPS are JSPS Research Fellows.

REFERENCES

1. T.R. Klassen, Nucl. Phys. **B** Proc. Suppl. **73** (1999) 918, hep-lat/9809174.
2. T.R. Klassen, unpublished.
3. T.R. Klassen, Nucl. Phys. **B533** (1998) 557.
4. A.X. El-Khadra, A.S. Kronfeld and P.B. Mackenzie, Phys. Rev. **D55** (1997) 3933.
5. P. Chen, hep-lat/0006019.